Received July 14, 2020, accepted August 1, 2020, date of publication August 5, 2020, date of current version August 17, 2020.

Digital Object Identifier 10.1109/ACCESS.2020.3014373

Numerical Simulation of Intermediate-Frequency Vacuum Arc

ZIANG TONG[1], JIANWEN WU[1], (Senior Member, IEEE), AND KUI LI[2]
[1]School of Automation Science and Electrical Engineering, Beihang University, Beijing 100083, China
[2]State Key Laboratory of Reliability and Intelligence of Electrical Equipment, Hebei University of Technology, Tianjin 300130, China

Corresponding author: Jianwen Wu (wujianwen@buaa.edu.cn)

This work was supported in part by the National Natural Science Foundation of China under Grant 51937004 and Grant 51677002; in part by the Civil Aircraft Special Research and Technology Research Project under Grant MJ-2017-S-46; and in part by the State Key Laboratory of Reliability and Intelligence of Electrical Equipment of Hebei University of Technology under Grant EERIKF004.

ABSTRACT With the development of more/all electric aircraft technology, variable frequency (360–800 Hz) power systems have become an important development focus for future aircraft design. Vacuum switches are highly suitable applications in this aviation power supply environment due to their excellent interrupting ability and reliability. In this paper, vacuum arc behaviors at intermediate frequencies were analyzed, and a numerical model of an intermediate-frequency (IF) vacuum arc was established. The plasma parameters and arc voltage characteristics were investigated. The regularities of arc voltage, ion temperature, ion density and plasma pressure during the arcing cycle were obtained, and the influence of the frequency and amplitude of the current on arc voltage characteristics and plasma parameters were analyzed. The correlations among the peak arc voltages and plasma parameters with the amplitude and the frequency of the current were determined. The results showed that the plasma parameters and arc voltages of the IF vacuum arc were obviously affected by the frequency and amplitude of the current at 2.5–7.5 kA. The simulation results were in good agreement with the experimental results, which proved the validity of this IF vacuum arc model.

INDEX TERMS Intermediate-frequency, vacuum arc, numerical model, plasma parameters, arc voltage characteristics.

I. INTRODUCTION

The increasing demands on the world's energy reserves and the continuous growth of the aviation industry have encouraged the aircraft manufacturers to move toward more/all electric solutions. This change has also led to a sharp increase in aircraft power generation capacity. As a mainstream civil aircraft, the Boeing B737NG has a generating capacity of 270 kVA, while the Boeing B787's capacity surges at 1,500 kVA [1], [2]. In this case, the traditional ''constant speed constant frequency'' mode and ''variable speed constant frequency'' mode are unable to meet the increasing power demands of more/all electric aircraft power supply systems in terms of power supply characteristics, reliability, maintainability and weight. The ''variable speed and variable frequency'' mode, in which the generator of the power supply system is directly driven by the engine accessory casing, has a simplified power generation system structure, strong maintainability, and large capacity and power density; this mode has greatly improved the power generation efficiency and reliability of aircraft power systems. In modern aircraft power supply systems, such as the Airbus A380, A350 and Boeing B787, the ''variable speed and variable frequency'' mode has been applied [3].

This increase in frequency leads to a significant increase in di/dt when the current crosses zero. It is difficult for a traditional air switch to meet the demand in an aircraft IF power supply system with increasing capacity. A vacuum switch uses vacuum as an arc extinguisher and offers the features of strong interrupting capacity, extremely high service life, reliability and safety [4], [5]. Given its excellent performance, it is highly suitable for application in an aviation power supply environment, which is extremely sensitive to air pressure and temperature. Therefore, to better apply vacuum switches to an aviation power supply system, it is necessary to study the vacuum arc voltage characteristics and plasma parameter characteristics at intermediate frequencies.

The associate editor coordinating the review of this manuscript and approving it for publication was Xiao-Jun Yang.

At present, most of the numerical simulation research on vacuum arc models has focused on 50/60 Hz frequencies. Boxman analyzed a vacuum arc as a fluid for the first time [6]. Keidar and Beilis *et al*. established a two-dimensional magneto hydrodynamics (MHD) model by combining the fluid equation with the electromagnetic equation [7]. A vacuum arc model established by Schade and Shmelev contained an energy conservation equation of electrons and ions [8]. Wang Lijun established an MHD model considering the effects of ion kinetic energy and viscosity [9].

The present research on IF vacuum switches has been mainly based on experiments, as there are few reports on the numerical modeling of vacuum arcs at intermediate frequencies. The breaking capacity, arc characteristics and contact ablation of an IF vacuum arc in cup-shaped axial magnetic field (AMF) contacts were obtained in [10]. The influence of the material and diameter of the AMF contacts on the arc characteristics and breaking performance at intermediate frequencies was obtained in [11]. The arc characteristics and the arc energy loss under transverse magnetic field (TMF) contacts at 50 Hz and 7 kHz were evaluated in [12]. In [13], the vacuum arc behavior and arc voltage characteristics of cup-shaped TMF contacts at intermediate frequencies were studied. A new contact with a curved surface was proposed to improve the current-interrupting ability, and the arc voltage characteristics, arc energy, ablation of the anode contact and condensation of the arc products at intermediate frequencies were investigated [14]. In [15], the plasma parameters of an IF vacuum arc at a current of 8.1 kA were measured by colorimetric thermometry. The reignition after interruption of intermediate-frequency vacuum arc was studied in [16].

For an IF vacuum arc with an extremely wide frequency range from 360 Hz to 800 Hz, the current vacuum arc simulation model has a complex algorithm and requires a long calculation time. To address the need for a simulation calculation of an IF vacuum arc and obtain the vacuum arc characteristics at multiple frequency points with less time cost, this paper established a numerical model of a vacuum arc at intermediate frequency. With this simulation model, arc voltage characteristics and plasma parameters at intermediate frequency during the arcing cycle were obtained, and the influence of the frequency and the amplitude of the current on arc voltage characteristics and plasma parameters were achieved.

II. EXPERIMENTAL RESEARCH ON VACUUM ARC BEHAVIOR AT INTERMEDIATE FREQUENCY

A. EXPERIMENTAL SYSTEM SETUP

The single-frequency oscillation circuit shown in figure 1 is used to study the intermediate-frequency vacuum arc. C_0, VT_0, L_0, VI constitute the main oscillation circuit. C_1, VT_1 and R_1 constitute an arc-starting circuit with a small value of approximately 90A until the contacts are fully opened. By adjusting C_0 and L_0 of the main circuit, the frequency of the current can be changed within the range of 360–800 Hz.

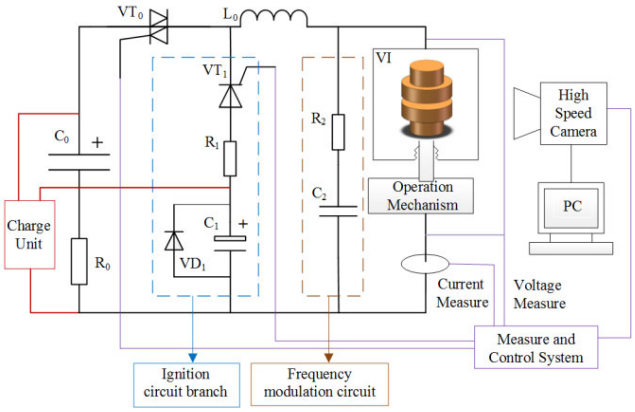

FIGURE 1. Schematic diagram of the IF circuit experimental system.

R_2 and C_2 are adjust the rate of rise of recovery voltages (RRRV) parameters. In the experiment, the recovery voltage can be 325–550 V for similarity to a 230 V aircraft power supply system. In present experiments, a 41 mm-diameter copper butt contact is selected. The gap distance is set to 3 mm, and the opening speed of electrodes is about 0.4–0.5 m s^{-1}. The vacuum chamber is able to maintain an internal pressure less than 5×10^{-4} Pa.

The contacts are separated at the starting circuit, and only at the full contact gap is the high current switched on. The experimental setup is different from that used in the actual circuit breaker (CB), which easily compares the IF vacuum arc behavior and other experimental results at different currents and frequency and reduces the uncertainty of the experiment. A digital oscilloscope can be used to record the arc voltage and the arc current measured by a Rogowski Coil. A high speed camera was used to record arc images. This camera was able to capture images at a speed of 35,087 frames per second with a resolution of 320 × 240.

B. ARC APPEARANCE AND DISCUSSION

An IF vacuum arc at a current of 2.5–7.5 kA was interrupted in the IF circuit experimental system. Fig. 2 shows the arc shape of the 5 kA vacuum arc at intermediate frequency. Since arc column plasma is basically emitted from the cathode spots along the opening distance, we determine the diameter of the arc by observing the range of the cathode spots. The arc behavior of the vacuum arc was divided into two stages in this paper: an expansion mode and a diffusion mode. In the expansion mode, with increasing arc current, the vacuum arc expands from the starting position to the surrounding area as new cathode spots are generated in the arc root area. The arc diameter increases approximately at the rate of current increase. The arc diameter reaches the peak value as the arc current is near the peak. The IF vacuum arc is in the diffusion mode as the arc current is in the descending phase. The diameter of the vacuum arc does not change obviously due to the gradual weakening of the cathode expansion. The observed result from the CCDs is that the cathode spots gradually decrease in brightness until they are extinguished.

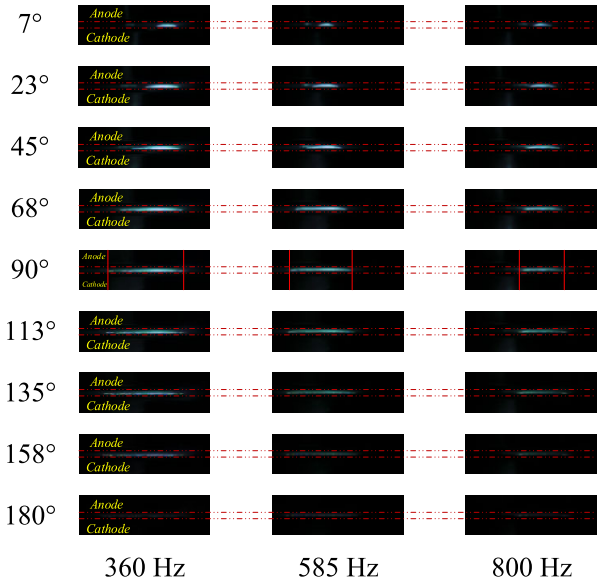

FIGURE 2. The IF vacuum arc behavior at a 5 kA peak current.

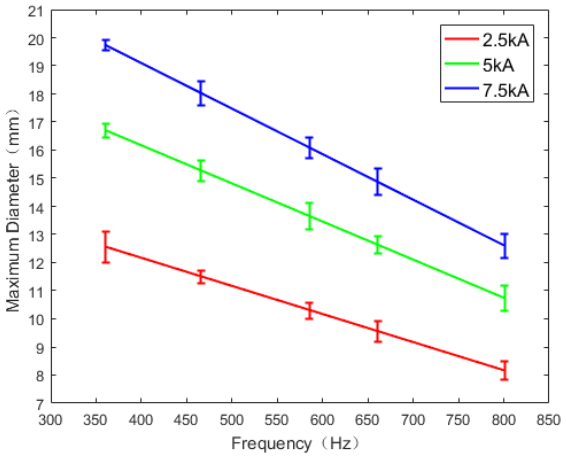

FIGURE 3. The maximum diameter of the IF vacuum arc at 2.5–7.5 kA peak current.

To gain the shape parameters of the simulation arc model, a correlation of the diameter of the vacuum arc changing with time during the whole arcing cycle is constructed. In order to prevent the discontinuity of the vacuum arc between the expansion mode and the diffusion mode, the correlation is constructed by using a sigmoid activation function:

$$D(t, I_{\mathrm{p}}, f) = \frac{D_{\max}(I_{\mathrm{p}}, f) \cdot \sin(2\pi f \cdot t)}{1 + e^{K \cdot (t - 1/4f)}} + \frac{D_{\max}(I_{\mathrm{p}}, f)}{1 + e^{-K \cdot (t - 1/4f)}} \tag{1}$$

where $D(t, I_{\mathrm{p}}, f)$ is the instantaneous diameter, mm; $D_{\max}$ is the maximum vacuum arc diameter, mm; I_{p} is the peak value of the arc current, kA; f is the current frequency, Hz; and K is 6000 in this paper.

As shown in Fig. 3, the maximum diameter during the arcing cycle is affected by the current frequency and amplitude. The larger the current amplitude is, the more cathode spots are needed. The variation of frequency will change the length of time when the vacuum arc is in the expansion mode.

When the current amplitude is constant, the maximum arc diameter decreases linearly with increasing frequency. It can be expressed by the following equation:

$$D_{\max}(I_{\mathrm{p}}, f) = D_0 \cdot I_{\mathrm{p}}^{\alpha} \cdot f + K_0 \cdot I_{\mathrm{p}}^{\beta} \tag{2}$$

where $D_{max}(I_{\mathrm{p}}, f)$ is maximum vacuum arc diameter, mm; I_{p} is the peak value of the arc current, kA; f is the current frequency, Hz. The parameters D_0 and K_0 are related to the contact structure and contact diameter, and the parameters α and β are related to the current, frequency and contact parameter. Typical values for D_0, K_0, α, and β are obtained by the twice linear least squares method at 2.5–7.5 kA at 360 Hz, 465 Hz, 585 Hz, 660 Hz, and 800 Hz frequencies; $D_0 = -6.680 \times 10^{-3}$, $K_0 = 11.03$, $\alpha = 0.4396$, and $\beta = 0.4174$.

III. ESTABLISHMENT AND ASSUMPTION OF MATHEMATICAL MODEL

At the moment of contact separation, the cathode contact surface of the vacuum interrupt is heated, and a large amount of metal vapor evaporates. The metal vapor is further ionized into positive ions and electrons to form an arc plasma. Based on the research of Rich and Farrall [17], this paper considered the generation, ionization, dispersion and condensation of metal vapor particles during the arc ignition process and established a numerical model of the IF vacuum arc.

Assumptions of the model in the simulation process are given as follows:

a. The IF vacuum arc is a symmetrical cylinder at small gap distance, the plasma parameters are uniform, and the effect of the magnetic field on the plasma parameters is neglected;

b. The solution region satisfies the quasi-neutral equation, $n_{\mathrm{e}} \approx z_{\mathrm{i}} \times n_{\mathrm{i}}$, where n_{e} is the electron number density, n_{i} is the ion number density, and z_{i} is the ion mean charge number;

c. The metal vapor particles, charged ions and electrons in the IF vacuum arc are considered to be in thermal equilibrium;

d. The anode is not active during the arcing cycle, and the evaporation of the anode is ignored. All the electrons in the IF vacuum arc are ionized by metal vapor particles.

e. The polar voltage drop is slightly affected by the frequency, and the energy exchange in the polar region does not affect the plasma parameters in the arc column region.

The metal vapor vaporized from the cathode is partly ionized into ions and electrons and is either partly diffused out of the gap or condensed on the contact surface during the arcing cycle. The equilibrium equation for the number of particles can be written as:

$$V_{\mathrm{arc}} \frac{\mathrm{d}n(t)}{\mathrm{d}t} = \int \Gamma_{ev} \mathrm{d}S_e - \sum_i c_i \int \Gamma_i \mathrm{d}S_i \tag{3}$$

where $n(t)$ is the metal vapor density of the IF vacuum arc at time t, m^{-3}; V_{arc} is the volume of the IF vacuum arc in the contact gap, which is determined by formula (1), m^3; Γ_{ev} is the flux density of the metal vapor particles injected into the

IF vacuum arc by evaporation from the cathode surface per unit time, $s^{-1} \cdot m^{-2}$; Γ_i is the flux density lost through the side and upper and lower surfaces of the IF vacuum arc per unit time, $s^{-1} \cdot m^{-2}$; and c_i is the condensation coefficient on the side of the contact gap and the lower surface of the contact.

According to the theory of molecular motion [18], we can assume

$$\Gamma_i = \frac{n(t)v}{4}, \quad v = \left(\frac{8kT}{\pi M}\right)^{0.5} \tag{4}$$

v represents the thermal velocity of metal vapor particles in the electrode gap; k is Boltzmann's constant; T is the temperature of the metal vapor particles in the IF vacuum arc; and M is the atomic mass of a metal vapor particle. The evaporation of metal particles is related to the current and corrosion rate, and the following equation can be obtained:

$$\frac{\int \Gamma_{ev} dS_e}{V} = \frac{\gamma}{MV} \cdot i(t) \tag{5}$$

$$i(t) = I_p \sin(2\pi f \cdot t + \varphi) \quad f : 360\text{Hz}\sim800\text{Hz} \tag{6}$$

γ represents the corrosion rate of the electrode, which is related to the contact material; as the experimental object of this numerical simulation model is the IF alternating vacuum arc obtained by igniting a DC arc, the initial phase angle φ is 0°. Taking $\gamma/MV = K_e$, we can rewrite (3) as

$$\frac{dn(t)}{dt} + \frac{v\sum_i c_i \int dS_i}{4V} \cdot n(t) = K_e I_p \sin(2\pi f \cdot t) \tag{7}$$

By solving (7), the function of the density and the pressure of the metal vapor in the IF vacuum arc changing with time during the arcing cycle is obtained:

$$n(t) \approx \frac{K_e I_p\left(\frac{v\sum_i c_i \int dS_i}{4V_{arc}} \cdot \sin\omega t - \omega\cos\omega t\right)}{\left(\frac{v\sum_i c_i \int dS_i}{4V_{arc}}\right)^2 - \omega^2} \cdot \left(1 - e^{-\frac{v\sum_i c_i \int dS_i}{4V_{arc}} \cdot t}\right) \tag{8}$$

$$V_{arc} = \pi\left(\frac{D(t, I_p, f)}{2}\right)^2 \cdot l_{arc} \tag{9}$$

$$P(t) = \frac{n(t) \cdot T \cdot P_0 \times 22.4 \times 10^{-3}}{273 \times 6.02 \times 10^{23}} \tag{10}$$

In order to facilitate the solution process of the equation, we assume the plasma temperature T and the volume of arc V_{arc} are constants before (8). After the expression of the ion density is obtained as (8), we consider T and V_{arc} as time variables. This approximation will cause a certain error in the solution of the ion density. Metal particles at high temperatures and pressures collide and ionize ions and electrons. The dissociation in the IF vacuum arc is characterized by the Saha formula as follows [19]:

$$\frac{\chi^2(t)}{1 - \chi^2(t)} = \frac{K_0 T^{2.5}(t)}{\overline{P}(t)} \exp\left(-\frac{11600 U_i}{T(t)}\right) \tag{11}$$

$\chi(t)$ is the ionization rate of the metal vapor; U_i is the ionization potential, which is related to the contact material; $n_e(t)$ is the electron density, where $n_e(t) \approx z_i \times n(t) \times \chi(t)$. Since only the electron current is considered, the electronic conductivity $\sigma(t)$ can be expressed by the following equation:

$$\sigma(t) = \frac{e^2 n_e(t)}{m_e f_{ei}}, \quad f_{ei}(t) = \frac{(\ln\Lambda/10)\, Z_i n_e(t)(\text{m}^{-3})}{3.5 \times 10^{10} T_e^{1.5}(\text{eV})} \tag{12}$$

where f_{ei} is the electron collision frequency, ln Λ is the Kulun logarithm, and Z_i is the relative charge number. The conductance G_{col} of the arc column and arc voltage can be shown as:

$$G_{col}(t) = \frac{4\sigma(t) \cdot L_{arc}}{\pi D_{arc}^2}, \quad U_{arc} = U_{anode} + U_{cathode} + U_{col} \tag{13}$$

where L_{arc} is the length of the arc column of the vacuum arc; D_{arc} is the diameter of the arc column of the vacuum arc; and U_{anode}, $U_{cathode}$ and U_{col} are the voltage drops of the anode, cathode and arc column, respectively [4].

For each simulation step, the external power supply injects energy into the vacuum arc through the electrode as follows:

$$W_{input}(t) = U_{arc} I_{arc} \cdot \Delta t \tag{14}$$

where I_{arc} is the current of the IF vacuum arc. As the particles in the IF vacuum arc will dissipate outward through the boundary, the energy carried away by these particles constitutes the main part of the energy dissipated by the IF vacuum arc. W_s(t) represents the energy dissipated by other forms, such as radiation and conduction, and we assume this part accounts for 15% of the total dissipated energy basing on the results in [20]. Since the particles always follow the principle of energy balance, the difference ΔW between the input energy and the dissipated energy of each step is equal to the change in the internal energy of the IF vacuum arc. According to (16) and (17), we can obtain the variation of the energy in the arc column during the arcing time. The following formulas show the correlation:

$$W_{loss}(t) = \frac{3}{2} kT(t) \cdot \Gamma_{loss}(t) \cdot S_i \cdot \Delta t + W_s(t) \tag{15}$$

$$W_\Delta(t) = W_{input}(t) - W_{loss}(t) \tag{16}$$

$$W_{arc}(t) = W_{arc}(t-1) + W_\Delta(t) \tag{17}$$

As we assume the particles in the IF vacuum arc are considered to be in thermal equilibrium, we can get the temperature of plasma on the basis of the energy balance principle by (18). And then we can fix the temperature of plasma by (19) and (20).

$$T_{energy}(t) = \frac{2}{3} \cdot \frac{W_{arc}(t)}{KV \cdot n_e(t) \cdot (1 + \chi(t) \cdot z_i)} \tag{18}$$

$$T_{error}(t) = T_{energy}(t) - T(t) \tag{19}$$

$$T(t) = T(t) + \Delta T(t) \tag{20}$$

IV. CONDITIONS AND CALCULATION METHODS

A real electrode dimension is adopted in this model. The electrode diameter is selected to be 41 mm, the material is pure copper, and the electrode separation is 3 mm. We selected a cathode erosion rate γ of 115 μg/C and an ionization

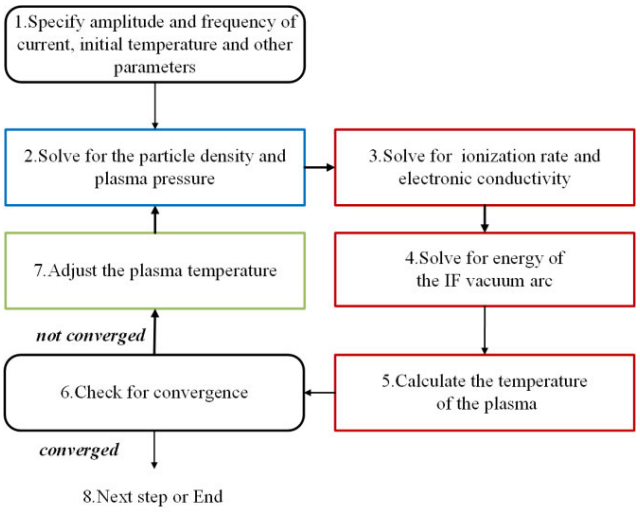

FIGURE 4. The calculation method of the vacuum arc numerical model at intermediate frequencies.

potential U_i of 7.72 V [21]. From Kutzner and Miller's experimental results [22], the mean charge number of ions z_i was 1.85. We found that the sum of the voltage drops of the anode and cathode is almost unaffected by the frequency at a current of 2.5–7.5 kA in our experimental conditions, and in this article, we consider it 14.2 V based on the average results of the experiment.

In this paper, the numerical model is designed to determine the plasma parameters and arc voltages of the IF vacuum arc during the arcing cycle. The solution method is as follows:

As is shown in Fig. 4, the first step is to set the peak value and frequency of the IF current. According to (6) and (9), the current amplitude and arc column volume during the arcing time can be determined. Based on experimental measurement results in [15], the initial value of the IF plasma temperature T is set. In the second step, the density and pressure of the particles in the arc column are solved by (8) and (10). Next, the ionization rate of the metal particles and the electronic conductivity of the arc column can be calculated by (11) and (12). According to (13) to (17), the energy in the arc column can be obtained by calculating the input and loss of arc energy. The fifth set is to calculate the temperature of plasma T_{energy} by (18) based on the energy balance. And then we need to judge whether the initial temperature T meets the solution requirements according to (19). If the difference between T_{energy} and the initial temperature T is within the allowable range, we believe that the plasma temperature T is reasonable, and then proceed to the next time step of the arcing time. If the difference between T_{energy} and the initial temperature exceeds the allowable range, we believe that initial temperature does not meet the balance of arc energy, and adjust the initial plasma temperature T in step 7 and repeat steps 2 to 5 again. It should be noted that the allowable range and the adjust size of plasma temperature ΔT needed to be set at the first step, and this setting will affect the calculation accuracy and calculation time.

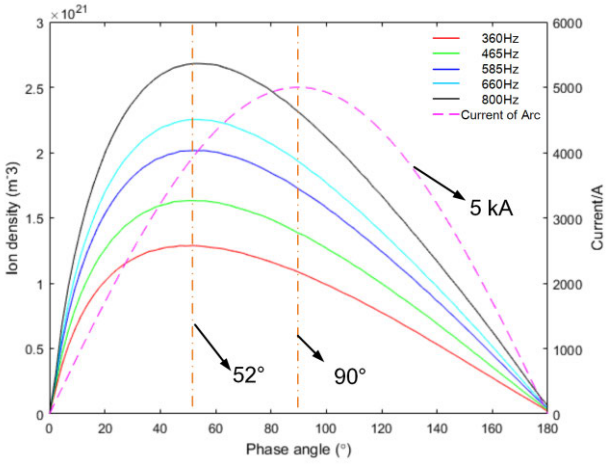

FIGURE 5. Ion density of 5 kA current at 360–800 Hz during the arcing cycle.

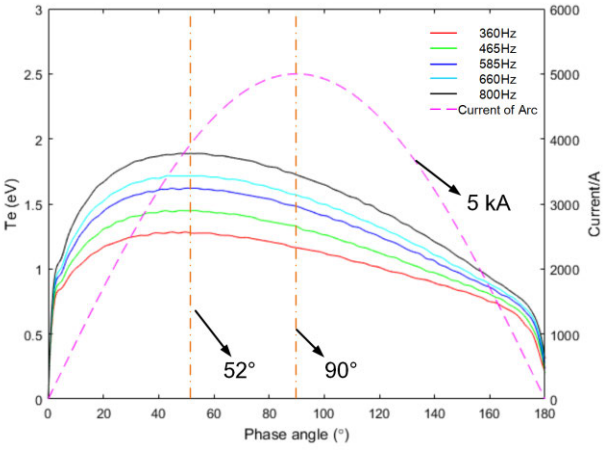

FIGURE 6. Ion temperature of 5 kA current at 360–800 Hz during the arcing cycle.

The above steps are carried out until the end of the entire arcing cycle.

V. SIMULATION RESULTS AND ANALYSIS

A. EFFECT OF FREQUENCY ON PLASMA PARAMETERS AND ARC VOLTAGE

The variation trend of the ion density of the vacuum arc at a current of 5 kA and frequencies of 360 Hz, 465 Hz, 585 Hz, 660 Hz, and 800 Hz is shown in Fig. 5 during the arcing cycle. The peak value of ion density ranges from 1.23×10^{21} m^{-3} to 2.68×10^{21} m^{-3}. The higher the frequency of the vacuum arc is, the higher the ion density is.

Fig. 6 and Fig. 7 show the plasma temperature and pressure of the IF vacuum arc at a current of 5 kA. The peak value of plasma temperature ranges from 1.24 eV to 1.83 eV, and the peak value of plasma pressure ranges from 0.75 kPa to 2.3 kPa.

When the current frequency is increased, the temperature and pressure reached in the IF vacuum arc are also higher, which is unfavorable for extinguishing the vacuum arc. Experimental studies have found that the vacuum arc

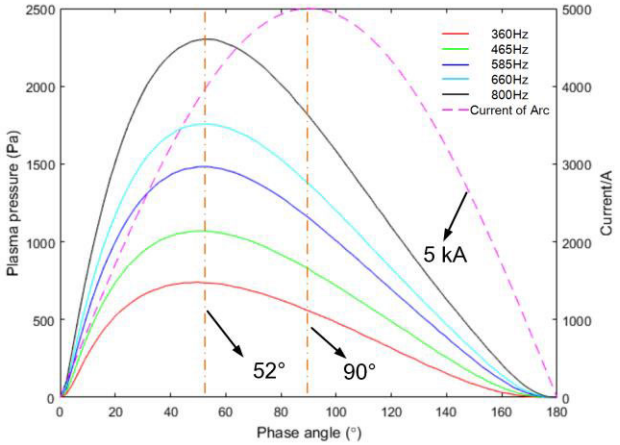

FIGURE 7. Plasma pressure of 5 kA current at 360–800 Hz during the arcing cycle.

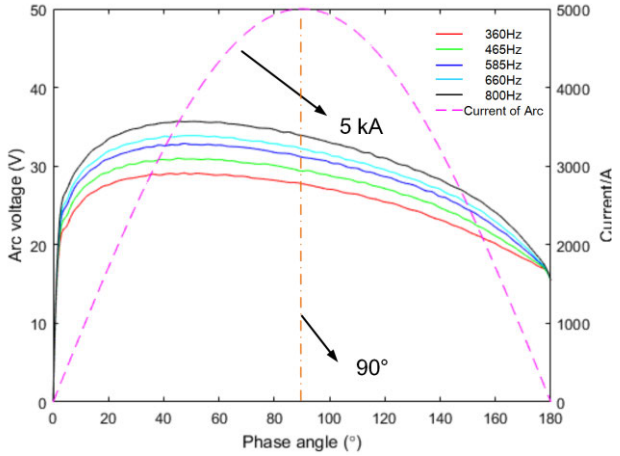

FIGURE 8. Arc voltage of 5 kA current at 360–800 Hz during the arcing cycle.

is more difficult to interrupt as the frequency increases at 360–800 Hz [10], [14].

As shown in Fig. 8, the arc voltage increases rapidly and then decreases slowly. The peak arc voltage increases with increasing frequency.

B. EFFECT OF AMPLITUDE ON PLASMA PARAMETERS AND ARC VOLTAGE

Figs. 9, 10, 11, and 12 show the variation trend of ion density, plasma temperature, ion pressure and arc voltage during the arcing cycle in a vacuum arc with amplitudes of 5 kA and 7.5 kA at 360 Hz and 800 Hz. The ion density, plasma temperature, ion pressure and peak arc voltage in the vacuum arc all increase with increasing current amplitude. The vacuum arc with currents of 800 Hz and 7.5 kA has the highest parameters. Among them, the peak ion density of the vacuum arc reaches 3.62×10^{21} m^{-3}, the peak ion temperature reaches 2.21 eV, the peak ion pressure reaches 3.67 kPa, and the peak arc voltage reaches 37.8 V. We found that as the current increases, more conducting particles are needed to conduct the current, which has a more obvious effect on ion density

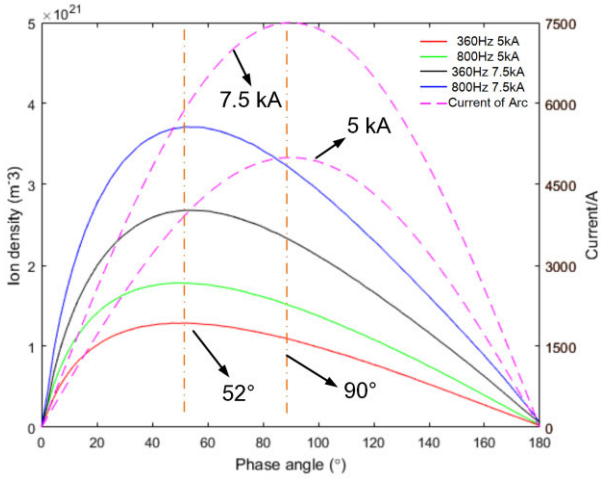

FIGURE 9. The ion density of 5 kA and 7.5 kA current at 360 Hz and 800 Hz during the arcing cycle.

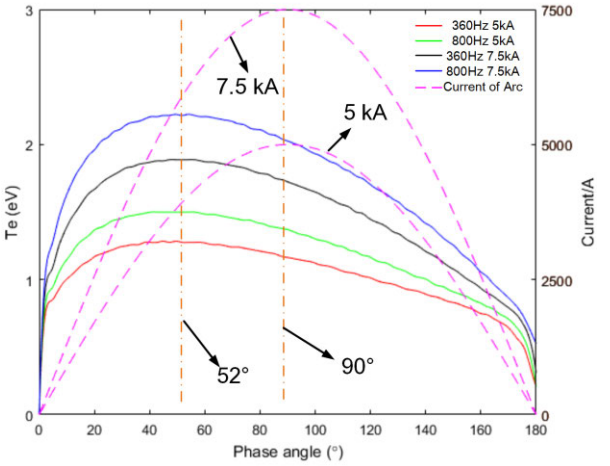

FIGURE 10. The ion temperature of 5 kA and 7.5 kA current at 360 Hz and 800 Hz during the arcing cycle.

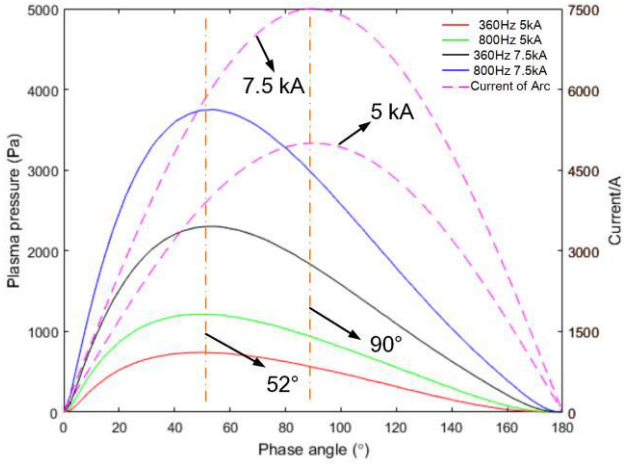

FIGURE 11. The plasma pressure of 5 kA and 7.5 kA current at 360 Hz and 800 Hz during the arcing cycle.

than the variation of arc volume caused by the improvement of current amplitude.

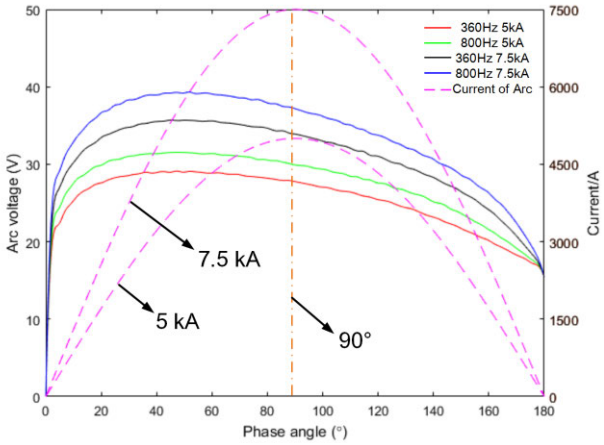

FIGURE 12. Arc voltages of 5 kA and 7.5 kA current at 360 Hz and 800 Hz during the arcing cycle.

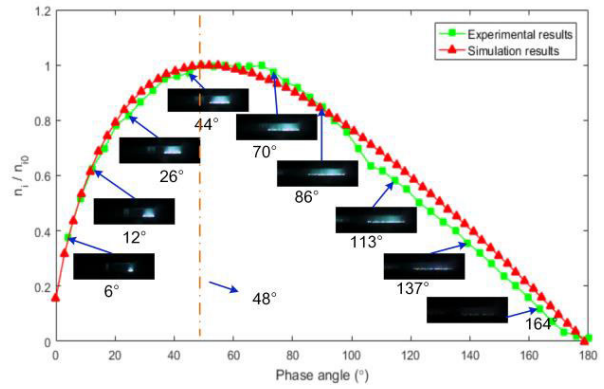

FIGURE 13. Comparison of simulation results and experimental results of vacuum arc ion density of 5 kA current at 800 Hz during the arcing cycle.

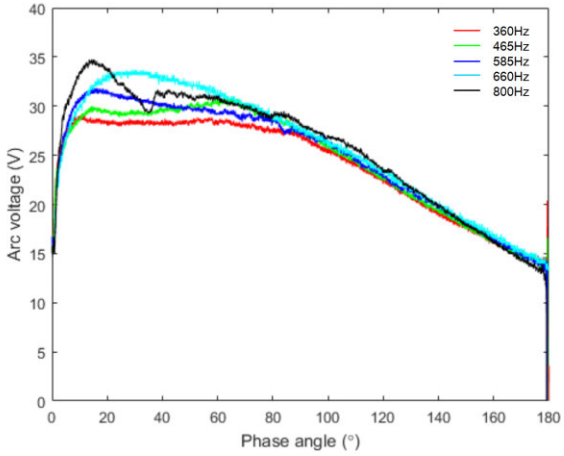

(a) Experimental results

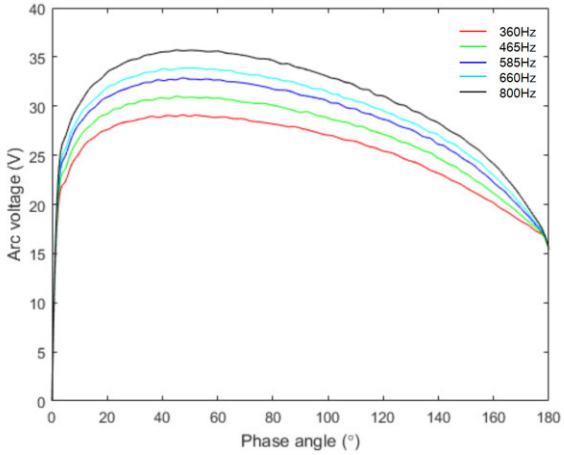

(b) Simulation results

FIGURE 14. Comparison of simulation results and experimental results of arc voltage of 2.5–7.5 kA current at 360–800 Hz.

C. COMPARISON BETWEEN SIMULATION RESULTS AND EXPERIMENTAL RESULTS

The light intensity of the vacuum arc observed by CCD is approximately positively correlated with the ion density [23], [24]. Therefore, images taken by a high-speed camera can verify the correctness of the trend of ion density in the simulation results during the arcing cycle. Video images of the vacuum arc under the 41 mm diameter copper electrode at 360 Hz 5 kA were analyzed and averaged to obtain the trend of the ion density in the IF vacuum arc during the arcing cycle, and they were compared with the simulation results. The two kinds of data were normalized, as shown in Fig. 13. In order to reflect the brightness change of the IF vacuum arc, the vertical height of the images were increased by 4.5 times. The simulation results are in good agreement with the variation trend of the measured results during the arcing cycle.

In [15], the arc temperature and electron density of an IF vacuum arc of 8.2 kA at 400 Hz, 650 Hz and 800 Hz were experimentally determined by using a two-band narrow-band continuous spectral measurement. The measured results showed that the temperature ranged from 0.5 eV to 2.5 eV, and the electron density ranged between 5.5×10^{20} m^{-3} and 2.1×10^{21} m^{-3}. These results were similar to the simulation results in this paper, and the measured plasma density tended to improve with increasing frequency, which was consistent with the conclusion obtained in this paper.

Fig. 14 shows a comparison of the simulation and experimental waveforms of the 5 kA arc voltage at 360 Hz, 465 Hz, 585 Hz, 660 Hz and 800 Hz. Since the arc voltage is affected by the random motion of the cathode spots, the arc voltage waveforms in the experiment show certain fluctuations. Fig. 15 shows a comparison of the simulation and experimental values of the arc voltage peaks of 2.5–7.5 kA at 360–800 Hz. The simulation results are in good agreement with the measured values, which indicates the effectiveness of the simulation model established in this paper.

VI. DISCUSSION

As shown in Fig. 5 and Fig. 13, the peak value of the ion density occurs before the peak of the arc current during the arcing cycle, whether in the simulation results calculated by the numerical model or the measured results by calculating the light intensity. In the initial phase of the arcing cycle,

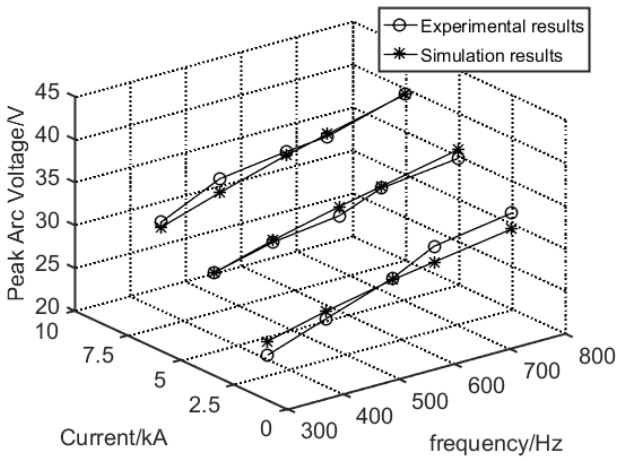

FIGURE 15. Comparison of simulation results and experimental results of peak values of arc voltage of 2.5–7.5 kA current at 360–800 Hz.

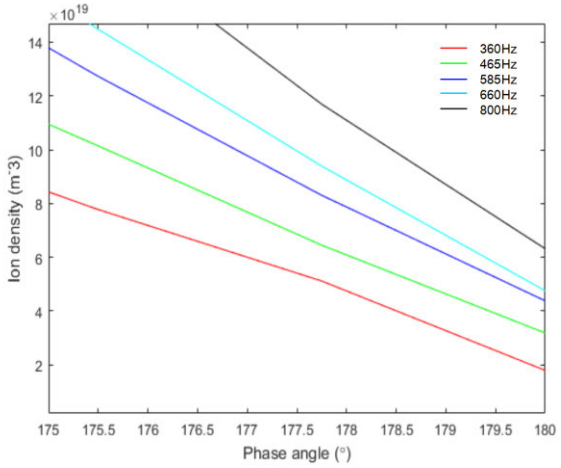

FIGURE 16. Ion density of 5 kA current at 360–800 Hz at 180° the arcing cycle.

due to the large current rise rate di/dt, the cathode injects ions and electrons into the IF vacuum arc at a faster speed. In addition, to quickly form a conductive plasma flow in the vacuum arc, a certain number of electrons and ions will rapidly accumulate in the arc plasma in a short time. At this time, the vacuum arc is still in the early stage of expansion. The increase in the volume of the IF vacuum arc is less than the accumulation of the number of ions, resulting in the density reaching a peak before the current peak. At the same time, the rapid increase in plasma density forces the vacuum arc to obtain more energy from the external circuit in a short time, which also leads to a rapid increase in arc voltage. In the experimental observations, the arc voltage often reaches its peak for the whole arc period at the beginning of the arcing cycle as shown in Fig. 14(a).

As is shown in figs. 5 and 16, the ion density is nearly zero at the phase angles of 0° and 180°. But the reason why it tends to 0 is different. In the perspective of analyzing the mathematical model of IF vacuum arc, the last term of equation (8) tends to zero at the phase angles of 0° and the first term of equation (8) tends to a relatively small value at the phase angles of 180°. In the perspective of analyzing the arc characteristics, there is no need to maintain abundant particles to deionize and conduct electricity in the arc column at the initial phase and at the end of arcing cycle as the current of arc is quite small at these moments. In addition, the value of the ion density at the phase angle of 180° implies the existence of residual plasma at current zero. This is consistent with the phenomenon in the experiments, and the ion density at current zero is similar to the calculations in [25]. The higher the density of residual plasma at current zero is, the more possible vacuum arc reignites after current zero under the influence of a transient recovery voltage (TRV) [4], [26]. As is shown in figure 16, the higher frequency of vacuum arc is, the higher the density of residual plasma at current zero. And this can explain why the higher-frequency arcs are easy to reignite in the experiments [14].

The influence of frequency on a diffuse arc at intermediate frequency is complicated. When the frequency is increased, the time length of the arc cycle will be reduced, the total energy injected into the arc gap by the external circuit will also be reduced, and the ablation on the electrode surface will be lighter. However, with an increase in frequency, the capacity of the vacuum arc to dissipate energy outward is also reduced due to the increase in the current change rate di/dt and the limited arc volume expansion speed, which leads to the accumulation of energy in the IF vacuum arc. The ion temperature and plasma pressure in the IF vacuum arc are greater at a higher frequency than at a lower frequency. This also leads to difficulty in interrupting the vacuum arc at high frequencies [14], [27].

According to the numerical model, the peak values of plasma parameters of 2.5–7.5 kA vacuum arcs with a frequency of 360–800 Hz are calculated, and the results and rules as shown in Fig. 16 can be obtained. According to Fig. 15 and Fig. 17, a similar correlation is found: the peak value of arc voltage, ion density, ion temperature and plasma pressure increases with current and frequency. The peak value of the arc voltage and plasma parameters have an approximately linear relationship with the frequency and amplitude of the current, and the following relationship is obtained:

$$\zeta(I_{\mathrm{p}}, f) = K_0 I_{\mathrm{p}} \cdot f + K_1 I_{\mathrm{p}} + K_2 f + \zeta_0 \tag{21}$$

where $\zeta(I_{\mathrm{p}}, f)$ is a physical quantity of voltage and plasma parameters related to the frequency and amplitude of the current; U_{pk} is the peak value of the arc voltage, V; $n_{\mathrm{i\_pk}}$ is the peak ion density, $10^{21}\mathrm{m}^{-3}$; $T_{\mathrm{e\_pk}}$ is the peak value of the ion temperature, eV; and P_{pk} is the peak plasma pressure, Pa. R^2 represents the correlation coefficient between the fitting parameters and the simulation results, and the correlation coefficients are all above 0.97. The coefficients of K_0, K_1, K_2 and ζ_0 are shown in Table 1, and their selection is related to the contact material, structure and electrode distance.

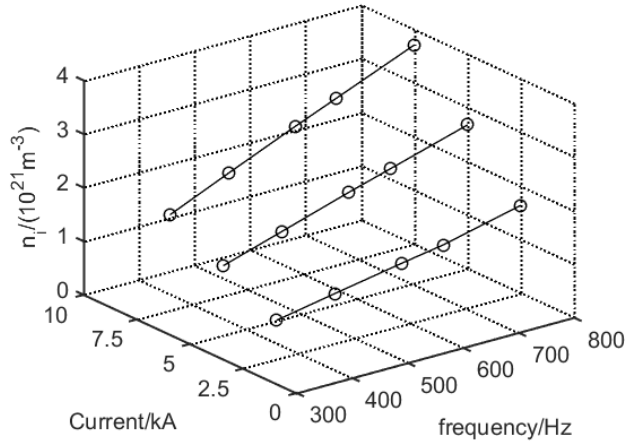

(a)Peak value of ion density

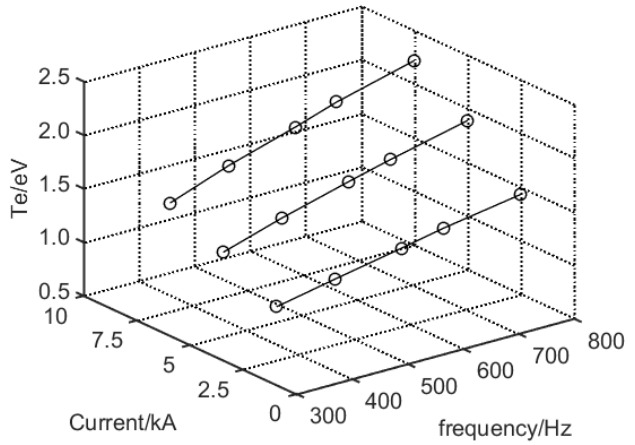

(b) Peak value of ion temperature

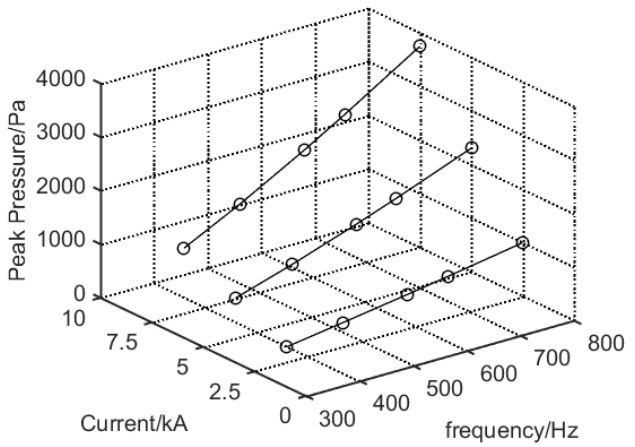

(c) Peak value of plasma pressure

FIGURE 17. Peak value of plasma parameters of 2.5–7.5 kA current at 360–800 Hz.

In the diffuse vacuum arc studied during the arcing cycle in this paper, no obvious aggregation phenomenon occurs. For the diffuse vacuum arc, the expansion of the arc is an important factor affecting the plasma parameters of the IF vacuum arc. The maximum value that the diameter of the arc can reach increases with increasing current amplitude. The experimental study in [14] shows that for the butt contacts, when the current is further increased to more than 10 kA, due to the randomness of the movement of the cathode locations and the self-generated magnetic field, the vacuum arc is easily diffused to the edge of the electrode, even at the side and back of the electrode. At this time, the violent sputtering of the arc plasma outside the gap will reduce the amount of IF vacuum arc plasma, and in order to balance the plasma density, more energy needs to be input from the outside, which causes the arc voltage to rise or emit high-frequency noise. To suppress this activity, it is also necessary to restrain the plasma by means of an axial magnetic field or by changing the structure of the electrode [14], [28].

TABLE 1. Coefficients in the formula for the peak value of arc voltage and plasma parameters of 2.5–7.5 kA current at 360–800 Hz.

ζ	K_0	K_1	K_2	ζ_0	R^2
U_{pk}/V	0.001104	1.11	0.009394	17.51	0.9763
$n_{i\_pk}/10^{21}m^{-3}$	0.000471	0.0462	0.000837	0.003263	0.9993
T_{e_pk}/eV	0.000126	0.0592	0.000696	0.5026	0.9942
P_{pk}/Pa	0.8301	-121.9	-0.5171	22.34	0.9987

VII. CONCLUSION

In this paper, through a simulation study of an IF vacuum arc, the following conclusions are obtained:

1) A numerical simulation model of an IF vacuum arc is established. The arc voltage obtained according to the numerical model simulation is in good agreement with the experimental results. The ion density and plasma temperature are close to the experimental measurement results.

2) Parameters such as IF vacuum arc ion density, plasma temperature, plasma pressure and arc voltage of an IF vacuum arc are greatly affected by the arc current frequency and amplitude. The higher the frequency and current amplitude are, the higher the waveform and peak value of each parameter are. The correlation of the peak value of arc voltage and plasma parameters with the amplitude and the frequency of the current is obtained.

3) The parameters such as ion density, plasma temperature, plasma pressure, and arc voltage of the IF vacuum IF vacuum arc during the arcing period increase rapidly at the initial stage and then slowly decrease. The peak of each plasma parameter appears before the arc current reaches the peak.

4) One reason that the IF vacuum arcs with higher frequency are easy to reignite is that they have higher plasma density at current zero.

5) The maximum value of arc diameter is affected by the current frequency and the current amplitude, which decreases with increasing frequency and increases with increasing amplitude. The correlation of the instantaneous value of arc diameter with arcing time is obtained at 2.5–7.5 kA and 360–800 Hz.

REFERENCES

[1] P. Wheeler and S. Bozhko, "The more electric aircraft: Technology and challenges," *IEEE Electrific. Mag.*, vol. 2, no. 4, pp. 6–12, Dec. 2014. [Online]. Available: https://ieeexplore.ieee.org/document/7008830
[2] P. W. Wheeler, J. C. Clare, A. Trentin, and S. Bozhko, "An overview of the more electrical aircraft," *Proc. Inst. Mech. Eng., G, J. Aerosp. Eng.*, vol. 227, no. 4, pp. 578–585, Apr. 2013, doi: 10.1177/0954410012468538.
[3] V. Madonna, P. Giangrande, and M. Galea, "Electrical power generation in aircraft: Review, challenges, and opportunities," *IEEE Trans. Transport. Electrific.*, vol. 4, no. 3, pp. 646–659, Sep. 2018.
[4] J. Wang, *Vacuum Switch Theory and Application*. Xi'an, China: Xi'an Jiaotong Univ. Press, 1986, pp. 49–53.
[5] Z. Liu, S. Cheng, Y. Zheng, M. Rong, and J. Wang, "Comparison of vacuum arc behaviors between axial-magnetic-field contacts," *IEEE Trans. Plasma Sci.*, vol. 36, no. 1, pp. 200–207, Feb. 2008. [Online]. Available: https://ieeexplore.ieee.org/document/4441771
[6] R. L. Boxman, "Magnetic constriction effects in high-current vacuum arcs prior to the release of anode vapor," *J. App. Phys.*, vol. 48, no. 6, pp. 2338–2345, 1977, doi: 10.1016/S0042-207X(77)80555-1.
[7] I. I. Beilis, M. Keidar, R. L. Boxman, and S. Goldsmith, "Theoretical study of plasma expansion in a magnetic field in a disk anode vacuum arc," *J. Appl. Phys.*, vol. 83, no. 2, pp. 709–717, Jan. 1998, doi: 10.1063/1.366742.
[8] E. Schade and D. L. Shmelev, "Numerical simulation of high-current vacuum arcs with an external axial magnetic field," *IEEE Trans. Plasma Sci.*, vol. 31, no. 5, pp. 890–901, Oct. 2003. [Online]. Available: https://ieeexplore.ieee.org/document/1240032
[9] L. Wang, S. Jia, Z. Shi, and M. Rong, "High-current vacuum arc under axial magnetic field: Numerical simulation and comparisons with experiments," *J. Appl. Phys.*, vol. 100, no. 11, 2006, Art. no. 113304, doi: 10.1063/1.2388734.
[10] J. Wang and J. Wu, "Experimental study of intermediate frequency vacuum arc under axial magnetic field," *Proc. CSEE*, vol. 29, no. 25, pp. 126–132, Sep. 2009. [Online]. Available: http://www.cnki.com.cn/Article/CJFDTotal-ZGDC200925023.htm
[11] Y. Jiang and J. Wu, "Effects of contact materials and diameters on characteristics of intermediate-frequency vacuum arc in axial magnetic field," *Proc. CSEE*, vol. 35, no. 20, pp. 5367–5374, 2015. [Online]. Available: http://en.cnki.com.cn/Article_en/CJFDTotal-ZGDC201520034.htm
[12] N. Hardt, M. Heimbach, H. Böhme, and D. Gentsch, "The dynamic voltage/current characteristics of vacuum arcs after breakdown at currents in the lower kHz-range," *Eur. T. Electr. Power*, vol. 12, no. 5, pp. 321–326, 2002, doi: 10.1002/etep.4450120502.
[13] Z. Liying, W. Jianwen, and Z. Xueming, "Arc movement of intermediate-frequency vacuum arc on TMF contacts," *IEEE Trans. Power Del.*, vol. 28, no. 4, pp. 2014–2021, Oct. 2013. [Online]. Available: http://ieeexplore.ieee.org/document/6570744
[14] Z. Tong, J. Wu, W. Jin, and J. Chen, "Properties of intermediate-frequency vacuum arc in sinusoidal curved contact and butt contact," *Plasma Sci. Technol.*, vol. 22, no. 2, Feb. 2020, Art. no. 024004. [Online]. Available: https:iopscience.iop.org/article/10.1088/2058-6272/ab519
[15] J. Wang and J. Wu, "Plasma characteristics of intermediate-frequency vacuum arc," *Proc. CSEE*, vol. 31, no. 36, pp. 145–152, Dec. 2011. [Online]. Available: http://en.cnki.com.cn/Article_en/CJFDTOTAL-ZGDC201136022.htm
[16] J. Yuan, W. Jianwen, and J. Bowen, "Reignition after interruption of intermediate-frequency vacuum arc in aircraft power system," *IEEE Access*, vol. 6, pp. 8649–8656, 2018. [Online]. Available: https://ieeexplore.ieee.org/document/8291144
[17] J. A. Rich and G. A. Farrall, "Vacuum arc recovery phenomena," *Proc. IEEE*, vol. 52, no. 11, pp. 1293–1301, Nov. 1964. [Online]. Available: https://ieeexplore.ieee.org/document/1445295
[18] T. L. Eddy, "Critical review of plasma spectroscopic diagnostics via MTE," *IEEE Trans. Plasma Sci.*, vol. PS-4, no. 2, pp. 103–111, Jun. 1976. [Online]. Available: https://ieeexplore.ieee.org/document/4316944
[19] V. Bakshi, "Saha equation for a two-temperature plasma," *Phys. Rev. A, Gen. Phys., Gen. Phys.*, vol. 42, no. 4, p. 2460, Aug. 1990, doi: 10.1103/physreva.42.2460.
[20] G. Zhang, *Electrical Appliances*. Beijing, China: China Mach. Press, 1980, pp. 48–50.
[21] C. W. Kimblin, "Erosion and ionization in the cathode spot regions of vacuum arcs," *J. Appl. Phys.*, vol. 44, no. 7, pp. 3074–3081, Jul. 1973, doi: 10.1063/1.1662710.
[22] J. Kutzner and H. C. Miller, "Integrated ion flux emitted from the cathode spot region of a diffuse vacuum arc," *J. Phys. D, Appl. Phys.*, vol. 25, no. 4, pp. 686–693, Apr. 1992, doi: 10.1002/ctpp.2150310302.
[23] L. Wang, S. Jia, Z. Shi, L. Zhang, and M. Rong, "Simulation analysis of influence of electrode separations on vacuum arcs characteristics under different states," *Proc. CSEE*, vol. 7, pp. 154–160, 2008. [Online]. Available: http://www.pcsee.org/en/y2008/v28/i7/154
[24] W. Shang, E. Dullni, H. Fink, I. Kleberg, E. Schade, and D. L. Shmelev, "Optical investigations of dynamic vacuum arc mode changes with different axial magnetic field contacts," *IEEE Trans. Plasma Sci.*, vol. 31, no. 5, pp. 923–928, Oct. 2003. [Online]. Available: https://ieeexplore.ieee.org/document/1240036
[25] S. E. Childs and A. N. Greenwood, "A model for DC interruption in diffuse vacuum arcs," *IEEE Trans. Plasma Sci.*, vol. PS-8, no. 4, pp. 289–294, Dec. 1980. [Online]. Available: https://ieeexplore.ieee.org/document/4317329
[26] E. Schade, "Physics of high-current interruption of vacuum circuit breakers," *IEEE Trans. Plasma Sci.*, vol. 33, no. 5, pp. 1564–1575, Oct. 2005. [Online]. Available: https://ieeexplore.ieee.org/document/1518979
[27] Z. Tong, J. Wu, H. Gao, X. Wang, J. Chen, Y. Jiang, and B. Jia, "Study on the characteristics of vacuum arc in sinusoidal curved contacts at intermediate frequency," *Proc. CSEE*, vol. 39, no. 21, pp. 6460–6470, Nov. 2019, doi: 10.13334/j.0258-8013.pcsee.190554.
[28] Y. Jiang, Y. Liu, Q. Li, J. Wu, J. Cui, and W. Zhang, "External excitation of axial magnetic field for intermediate-frequency vacuum arc research," *IEEE Access*, vol. 7, pp. 161088–161093, 2019. [Online]. Available: https://ieeexplore.ieee.org/document/8888170

ZIANG TONG was born in Liaoning, China, in 1991. He received the B.S. degree in electronic engineering from North China Electric Power University, Beijing, China, and the M.S. degree in electronic engineering from the North China University of Technology, Beijing. He is currently pursuing the Ph.D. degree in electrical engineering with Beihang University, Beijing. His research interests include theory and application of vacuum arcs, intelligent electrical apparatuses, and power electronics technology.

JIANWEN WU (Senior Member, IEEE) received the B.S. and M.S. degrees in electrical engineering from the Shenyang University of Technology, Shenyang, China, in 1984 and 1987, respectively, and the Ph.D. degree in electrical engineering from Xi'an Jiaotong University, Xi'an, China, in 1995. From 1995 to 1998, he was a Postdoctoral Fellow with the Huazhong University of Science and Technology, Wuhan, China. Since 2001, he has been a Faculty Member with the School of Automation Science and Electrical Engineering, Beihang University, Beijing, China, where he is currently a Professor. His research interests include theory of vacuum arcs, intelligent electrical apparatuses, and power electronics technology.

KUI LI was born in Baoding, Hebei, China, in 1965. He received the B.S. and M.S. degrees in electrical engineering from the Hebei University of Technology, Tianjin, China, in 1987 and 1992, respectively, and the Ph.D. degree in electrical engineering from Fuzhou University, Fuzhou, China, in 1996. He is currently a Professor with the School of Electrical Engineering, Hebei University of Technology. He has authored or coauthored over 100 technical articles and two monographs. His current research interests include reliability and intellectualization of electrical apparatus, fault diagnosis, and life prediction of electrical apparatus.